Frontiers in Bioscience Landmark

Front. Biosci. (Landmark Ed) **2025**; 30(7): 38726
https://doi.org/10.31083/FBL38726

Original Research

Bronchoalveolar Lavage Derived Fibroblasts From Interstitial Lung Disease Patients: A Chance to Exploit 2D/3D Model of Pulmonary Fibrosis *In Vitro*

Paolo Giannoni[1], Emanuela Barisione[2], Marco Grosso[2], Maria Bertolotto[3,4], Paola Altieri[5,6], Federico Carbone[3,4], Fabrizio Montecucco[3,4], Daniela de Totero[7,*]

[1]Department of Experimental Medicine, University of Genoa, 16132 Genoa, Italy
[2]Interventional Pulmonary Unit, IRCCS Ospedale Policlinico San Martino, 16132 Genoa, Italy
[3]First Clinic of Internal Medicine, Department of Internal Medicine, University of Genoa, 16132 Genoa, Italy
[4]Italian Cardiovascular Network, IRCCS Ospedale Policlinico San Martino, 16132 Genoa, Italy
[5]Cardiac Thoracic and Vascular Department, IRCCS Ospedale Policlinico San Martino,16132 Genoa, Italy
[6]Department of Internal Medicine, University of Genoa, 16132 Genoa, Italy
[7]Molecular Pathology Unit, IRCCS Ospedale Policlinico San Martino, 16132 Genoa, Italy
*Correspondence: daniela.detotero@hsanmartino.it (Daniela de Totero)

Academic Editor: Eun Sook Hwang
Submitted: 28 February 2025 Revised: 7 May 2025 Accepted: 22 May 2025 Published: 7 July 2025

Abstract

Background: Bronchoalveolar lavage (BAL) constitutes a valuable diagnostic approach for the differential diagnosis of various pulmonary fibrotic diseases. BAL fluids from patients with interstitial lung diseases (ILDs) can also be utilized for research purposes, offering cell populations suitable for functional and phenotypical studies. In this study, we demonstrate the feasibility of isolating a discrete number of fibroblasts/myofibroblasts *in vitro* from the BAL fluid from ILD patients, a procedure typically performed during the early stages of disease when high-resolution computed tomography does not yield a definitive diagnosis. **Methods**: We obtained BAL samples from a total of 43 patients. Fibroblasts were successfully derived *in vitro* from 20 patients, with larger quantities of cells from 11 patients. Whenever possible, the cells were cultured and expanded until passage 12–15. Fibroblasts could be expanded to passage 36 in only one case. The expression of typical fibrotic markers, such as type I collagen, α-smooth muscle actin, and fibronectin-extra domain A or B (FN-EDA/-EDB), was therefore compared in fibroblasts obtained from ILD-patients with fibroblasts derived from non-diseased controls by quantitative RT-PCR, immunofluorescence, and cytofluorographic analysis. The rate of proliferation, migration, and response to the anti-fibrotic drug pirfenidone was further determined in 2D and in 3D models of *in vitro* cultures. **Results**: A specific morphological heterogeneity among fibroblasts/myofibroblasts derived from patients with fibrotic or non-fibrotic ILD was observed, such as enlarged and flattened shaped cells *vs* spindle-shaped cells. Moreover, a higher expression of α-smooth muscle actin (α-SMA), type I collagen (collagen I), and fibronectin was demonstrated in ILD fibroblasts than in control fibroblasts. The anti-fibrotic drug pirfenidone was effective in inhibiting the growth and migration of ILD-fibroblasts both in 2D and 3D *in vitro* models. **Conclusions**: Collectively, the present study suggests that BAL-derived fibroblasts from ILD patients may serve as a useful *in vitro* model for studying and assaying pulmonary fibrosis. This approach has the potential to improve our understanding of ILD pathogenesis and overcome ethical and availability concerns associated with biopsy-derived tissues.

Keywords: interstitial lung diseases; bronchoalveolar lavage; fibroblasts; *in vitro* testing; pirfenidone

1. Introduction

Interstitial lung disease (ILD) is a large and heterogeneous group of diseases characterized by damage to the lung parenchyma due to the combination of inflammation and fibrosis. Idiopathic pulmonary fibrosis (IPF) is regarded as the prototype of fibrosing ILD. Idiopathic Pulmonary Fibrosis, which progressively displays fibrotic invasion and loss of lung function, has a poor prognosis, with a median survival of three years from diagnosis [1]. Not all ILD are associated with progressive fibrosis; those that develop this phenotype however display a clinical course similar to IPF [2]. Up to a third of ILD are estimated to develop advanced fibrosis [3]. Progressive fibrosis interstitial lung disease (PF-ILD) is not a clinical entity but describes a group of ILD with similar clinical behavior: this phenotype may occur in patients displaying different etiologies, and it is more frequently seen in hypersensitivity pneumonitis (HP), autoimmune diseases such as rheumatoid arthritis (RA) and systemic sclerosis (SS), idiopathic non-specific interstitial pneumonia (NSIP), and unclassifiable ILD, whereas it seems to be uncommon in others such as lymphoid interstitial pneumonia or organizing pneumonia [3–5]. A clear comprehension of the patho-biological mechanisms occurring in the different ILD appears therefore a challenge for correct diagnosis and treatment. Optimization of ILD diagnosis, other than requiring a mul-

tidisciplinary approach involving pulmonologists, radiologists, and pathologists, may include bronchoalveolar lavage (BAL) examination in clinical guidelines, further encouraging standardization of BAL procedures. Moreover, the cellular analysis of BAL is of great importance for diagnosing inflammatory and infectious processes occurring at the alveolar level, providing additional insights into the underlying pathogenic mechanisms [6].

In IPF, fibroblasts/myofibroblasts and epithelial cells (alveolar cells of type I–II) have emerged as the major players. Myofibroblasts accumulate in IPF lungs forming typical zones of collagen deposition called "fibroblastic foci" that, as the predominant sites of excess matrix production, can be thought of as the leading edge of active fibrosis [7,8]. These changes in the extracellular matrix (ECM) composition contribute to IPF progression leading to distortion of lung architecture and homeostasis. The multiple origins of the fibroblasts are however still a matter of debate, being possibly due to the proliferating resident fibroblasts, to epithelial-mesenchymal-transition of epithelial, endothelial, or mesothelial cells, or to circulating blood mesenchymal precursors migrating into the lung [9–11]. We have addressed here the possibility of deriving and expanding *in vitro* fibroblasts from the BAL of ILD patients. Although BAL-derived fibroblasts growing *in vitro* for a long time are not easy to obtain, this procedure can be of useful for research studies, further overcoming ethical concerns linked to the utilization of biopsy-derived tissues. In addition, while cells derived from lung biopsies are generally obtained from patients with late stage of disease, in this way it is also possible to obtain fibroblasts even from patients with early disease. Comparative analyses of fibroblasts derived from different ILD disorders may further shed new light on the pathogenesis as well as on molecular mechanisms underlying progressive pulmonary fibrosis. Here we further show how the possibility of managing discrete quantities of primary ILD-fibroblasts could be of interest to develop various models of 3D-cultures to better assess features of these cells in a more physiological system, and either to exploit pre-clinical testing of in-use, or novel, therapeutic agents. Multi-omics studies comparing fibroblasts/myofibroblasts from various ILD will be of further help to clarify the pathobiology of pulmonary fibrosis progression.

2. Materials and Methods

2.1 Patients: Clinical Features and Bronchoalveolar Fluid Collection

The present study was approved by the Institutional Ethics Committee of the IRCCS Ospedale Policlinico San Martino, Genoa, Italy (protocol code ILDFIBRO020, n. of Register CER Liguria: 523/2020 DB id 10931) and conducted according to the current national and international guidelines; within the study, biological samples were anonymized prior to processing. For patients the diagnosis was based on international criteria [12,13]. After multidisciplinary discussion of the Interstitiopathy Lung Disease (ILD) group of the case, and after signing an informed consent form, explicitly authorizing the use of biological samples and any derivative thereof for research purposes, the patient underwent a transbronchial cryobiopsy with bronchoalveolar collection for diagnostic purposes [14]. Aliquots of BAL fluid unused for diagnostic purposes (15–25 mL) were therefore processed for additional research procedures. The clinical features of the patients employed in this study are summarized in **Supplementary Tables 1,2**. The total lung capacity (TLC), forced vital capacity (FVC), forced expiratory volume in 1s (FEV1), and diffusing capacity (DL_{CO}) were measured according to international guidelines [12,13].

2.2 Culture of Bronchoalveolar Fluid, Fibroblasts Derivation and Expansion

Primary derived bronchial fibroblasts were derived from fresh ILD- bronchoalveolar lavage, 15 mL which is the small fraction normally left unused for routine diagnostic analyses. Cells of the BAL fluids were first pelleted by centrifugation. While supernatant was recovered and frozen for different types of investigations, cells were resuspended in 6 mL of complete medium (RPMI-1640 + 10% fetal calf serum (FCS); Lonza, Walkersville, MD, USA), seeded in a 24 well plate and cultured at 37 °C and 5% CO_2. Fibroblast growth factor 2 (FGF2; 3 ng/mL; Miltenyi Biotec GmbH, Bergisch Gladbach, Germany) was added 1 day after. The medium was changed once a week with the addition of FGF2. In some cases, after 2–3 weeks, a good number of spindle-shaped cells attached to the bottom of the well could be observed. These cells were therefore cultured until confluence, detached by the use of 1$\times$ trypsin-EDTA (Euroclone S.p.A., Pero, Milan, Italy), washed, collected and expanded in 24 or 6-well plates. As quickly as possible a small aliquot of cultured fibroblasts was used for RNA extraction to preliminarily assess the expression of specific fibroblasts/myofibroblasts markers (i.e., α-smooth muscle actin (α-SMA), type I collagen (collagen I), fibronectin) by quantitative RT-PCR analysis. In some cases fibroblasts could be further expanded until passages 10–12, thus allowing a deeper phenotypical/functional characterization, as well as the storage of many vials in liquid nitrogen. In one particular case we could expand the fibroblasts of one patient for a very long time (9 months) until passage 36, as we previously described (SCI13D) [2]. In addition, from the same patient, but out of a second BAL sample collected one year later, we also derived new additional fibroblasts. These however differed from the previous ones, missing the chromosome 10 trisomy that characterized the earlier fibroblasts. These cells were called SCI2 and could be expanded until passage 14.

2.3 Cell Lines or Primary Fibroblasts Used as Controls or to Derive Spheroids/Organoids

The MRC5 cell line (from Interlab Cell Line Collection "ICLC" IRCCS Ospedale Policlinico San Martino, Genoa, Italy), fibroblasts isolated from the lung tissue derived from a white male, 14-week-old embryo, was cultured in flasks in complete medium (RPMI+FCS10%) (Euroclone S.p.A). Cells reaching confluence were detached by trypsin 1X (Euroclone S.p.A), split or either frozen. Primary fibroblasts were further derived from the BAL of a patients with no evidence of pulmonary fibrosis while skin fibroblasts derived from a healthy subject were used as a further control.

We also utilized the A549 cell line (obtained from ICLC, IRCCS Ospedale Policlinico San Martino, Genoa, Italy) that, although derived from lung adenocarcinoma, is experimentally utilized as representative of alveolar basal epithelial cells [15]. We also used the human umbilical vein endothelial cell line HECV (from ICLC, IRCCS Ospedale Policlinico San Martino, Genoa, Italy). Both these cell lines were cultured as monolayer in flasks in RPMI+FCS 10%, detached when they reached 70% confluency by 1× trypsin -EDTA (Euroclone S.p.A.), and then re-cultured, frozen or employed in 3D models of cultures. All cell lines were validated by Short Tandem Repeat (STR) profiling and all the cells used were tested negative for mycoplasma.

2.4 Total mRNA Extraction and Quantitative Real-time PCR Assay

Briefly, cells were washed in a PBS solution (Euroclone S.p.A.), trypsinized and collected by centrifugation (400 ×g) and processed for mRNA extraction, according to the manufacturer's instruction of the GeneUP™ Total RNA Kit (BiotechRabbit GmbH, Berlin, Germany). A cDNA pool for each sample was then generated by using the SuperScriptTM III First-strand synthesis system for RT-PCR Kit (Invitrogen; Milan, Italy); a sybr-green RealMasterMix SYBR ROX 2,5X (5-Prime GmbH, Hamburg, Germany) was used in an Eppendorf Mastecycler Realplex2 apparatus, applying a real time quantitative RT-PCR analysis. Each reaction was performed in triplicate for each sample, according to the following settings: a single denaturation step at 95 °C for 3 minutes; 45 cycles at 94 °C for 30 sec, 60 °C for 30 sec, 72 °C for 40 sec, and a final step at 72 °C for 7 min. Reaction specificity was counterchecked by the melting curve analysis. The expression of each target gene was normalized to the endogenous housekeeping gene glyceraldehyde-3-phosphate dehydrogenase (GAPDH). Primer sets for target genes were purposely designed, as for the alpha Smooth Muscle Actin (α-SMA; forward primer: TGGAAAAGATCTGGCACCAC, reverse primer: CTCAAACATAATTTGAGTCAT), Fibronectin (FN; forward primer: TACACTGGGAACACTTACCG; reverse primer: CCAATCTTGTAGGACTGACC), fibroblast growth factor-2 receptor (FGF-2R; forward primer: AGACAGGTAACAGTTTCGGCT, reverse primer: CAGTGTCAGCTTATCTCTTGG), or derived from previously published sequences. Expression levels of target genes in the different samples/culture conditions were normalized by the levels of the corresponding gene in control samples/cultures.

2.5 Morphological, Cytofluorographic and Immunofluorescence Analysis

Morphological features of live cultured cells were examined under an inverted Olympus CKX-41 microscope (Olympus Corp., Tokyo, Japan); images were acquired using a Nikon Digital Sight DS-5Mc equipped with the NIS-Elements F2.20 software (Nikon Corp., Tokyo, Japan). Expanded fibroblasts were also analyzed for the expression of CD105, CD90, CD73, CD45, Vimentin, type I Collagen, α-SMA, fibronectin by cytofluorographic analysis. Phenotypical analysis was performed by staining detached cells with specific antibodies for membrane antigens such as anti-human-CD105-PE (Cat.n. 21271054), -CD73-FITC (Cat.n. 21270733), -CD90-APC (Cat.n. 21270906) or -CD45-FITC (Cat.n. 21270453) (all from Immuno-Tools GmbH, Friesoythe, Germany). After 30 min of incubation at 4 °C the cells were washed twice and resuspended in phosphate buffered saline (PBS)+ FCS 2%. For intracytoplasmic staining the cells were first fixed with 1% paraformaldehyde (PFA) and incubated in the dark at 4 °C for 15 min. After two washes with PBS+2% FCS the cells were permeabilized with a permeabilization solution (0.1% Na-citrate and 0.1% Triton in PBS 1×) and then stained with the anti-human-α-SMA antibody (clone 1A4, Sigma-Aldrich, St.Louis, MI, USA), or -procollagen 1 (SP1.D8; Developmental Studies Hybridoma Bank, University of Iowa; Iowa City, IA, USA) or -fibronectin (DP3060, ACRIS, Li-Starfish, Milan, Italy) and incubated on ice for 30 min. Cells were then washed and, after the addition of 50 µL of permeabilization solution, were stained with a specific anti-mouse or anti-rabbit secondary FITC or PE-conjugated antibody (Southern Biotechnology, Birmingham, AL 35226, USA), and incubated at 4 °C for 30 min. Cytofluorographic analysis was then performed using a FACS-Canto cytofluorimeter (Becton Dickinson; Franklin Lakes, NJ, USA).

To determine the expression of F-actin fibers by immunofluorescence, fibroblasts were cultured in eight-well chamber slides (Nunc International, Rochester, NY, USA) in a total volume of 300 µL of culture medium and then treated with transforming growth factor-β1 (TGF-β1; 5 ng/mL; D.B.A. Italia, Segrate, Milan, Italy), or Pirfenidone (300 µg/mL; D.B.A. Italia, Segrate, Milan, Italy), or TGF-β + Pirfenidone for 72 h. Cells were fixed in PFA 2.5%, permeabilized with Triton × 100, and stained with Alexa-Fluor 555-conjugated phalloidin (Thermo Fischer Scientific; Rodano, Milan, Italy). The expression of F-actin was then observed by fluorescence microscopy and im-

ages were acquired with a Hamamatsu C5810 color-chilled 3 CCD camera (Hamamatsu Photonics K.K., Hamamatsu City, Shizuoka, Japan). Identical camera settings (time of exposure, brightness, contrast, and sharpness) and an appropriate white balance set according to the fluorescence filter were used. Nuclei were counterstained with DAPI.

2.6 β-galactosidase (β-gal) Detection in Cultured ILD-fibroblasts

Fibroblasts were cultured in 24 well plates, washed with PBS 1× and then fixed with PFA 4% for 5 min at room temperature. Cells were rinsed with PBS and incubated overnight in the incubator at 37 °C in SA-β-gal staining solution containing: 1 mg mL^{-1} X-gal, 40 mM citric acid/sodium phosphate buffer pH 6.0, 5 mM potassium ferricyanide, 5 mM potassium ferrocyanide, 150 mM sodium chloride and 2 mM magnesium chloride in water. Cells were then rinsed with PBS and observed with an inverted bright field microscope and at least 5 Images for each well were acquired as described above.

2.7 Proliferation and Migration Assays

Available aliquots of cells, BAL-patients originated, were expanded in complete medium (RPMI + FCS10%), detached with Trypsin 1×, counted, re-seeded in 24-well plates to a density of 10^4 cells/mL in complete medium and left to adhere for 24 h. Non-adherent cells were washed away and treatments were performed by exposing cells to complete medium supplemented with TGF–β1 (5 ng/mL; Miltenyi Biotech), Pirfenidone (150–450 µg/mL; D.B.A. Italia), or both. At the scheduled time point cells were washed with sterile PBS and incubated for 4 h at 37 °C with complete culture medium supplemented with 10% Alamar Blue™ (Invitrogen; Milan, Italy). Aliquots of the supernatants were then drawn and assessed spectrophotometrically, at 570 and 600 nm, in a Spectra MR Dynex apparatus. Cells were then rewashed in PBS and replenished with complete medium. Determinations of the absorbance were performed in duplicate for each well and treatment, for each time-point (0, 1, 4 and 7 days), according to the manufacturer's suggestions.

Fibroblasts of different patients were also used to perform wound scratch tests; cells were seeded in 24-well plates to a density of 10^4 cells/mL, let adhere and proliferate to semi-confluency in complete/treatment medium. A sterile 200 µL-micropipette tip was then used to generate a scratch onto the full length of the cell layer, along the diameter of each well. Cells were then washed in PBS and treatments started by the addition of TGF-β1 (5 ng/mL) and/or Pirfenidone (150, 300 or 450 µg/mL), wherever needed. The number of cells encompassed within the lesion borders, at any assessed time point and treatment, was the parameter chosen to evaluate growth conditions among the experimental settings assessed. Images of cells filling the gaps of the same lesion site were acquired after 0, 12, 24, 36 and 48 h; the boundaries of each original lesion were then superimposed to frames captured from the same plate in the same position at the different experimental time point; cells falling within the lesion boundaries were then counted using the National Institute of Health ImageJ free-software 1.53 (https://imagej.net/ij).

2.8 Establishment of a 3D Model Growth of Fibroblasts, Epithelial (A549) and Endothelial (HECV) Cells as Spheroids or Organoids: Determination of Their Response to Pirfenidone Treatment

Using ultra-low attachment 96 well U bottom plates (Greiner Bio-One GmbH, Maybachstr 2, 72636 Frickenhausen, Germany) we further established 3D *in vitro* cultures of ILD-fibroblasts (Spheroids) or of ILD-fibroblasts together with epithelial/endothelial cells (Organoids). Spheroids and Organoids were then tested with Pirfenidone (D.B.A. Italia). To this aim 4000 ILD-fibroblasts or A549 or HECV (Spheroids) or either 2000 ILD-fibroblasts + 3000 A549 or HECV cells (Organoids), were re-suspended in 50 µL of complete medium (RPMI+FCS 10%), seeded in each well and then cultured in the incubator at 5% CO_2 and 37 °C for 48 h. After 48 h, 50 µL of complete medium with/without Pirfenidone were added. Pirfenidone was used at a concentration of 300 µg/mL in the final volume of 100 µL of culture medium for each well. After additional 72 h the images of each Spheroids or Organoids, treated or untreated with Pirfenidone, were acquired using a Nikon Digital Sight DS-5Mc as detailed above. Subsequently the size of untreated or treated spheroids or organoids was determined by measuring their visible area by means of the available tools of the free software Image J version 1.53.

2.9 Assessment of 3D Invasion Property of Fibroblasts Treated or Untreated With Pirfenidone

Analysis of invasion by spheroids in a 3D model was performed based on the procedures described by Dsouza KG and co-authors [16] with some modifications. Spheroids were preliminarily prepared as above described and cultured for 48 h in a CO_2 incubator at 37 °C. After 48 h pre-cooled collagen (PureCol EZgel; Advanced Biomatrix; Carlsbad, CA, USA) was first diluted with RPMI-1640 at a concentration of 1 mg/mL and gently mixed avoiding the formation of air bubbles. A volume of 50 µL/well of this solution was added to cover the layer of flat-bottom 96 well plates, subsequently incubated at 5% CO_2 and 37 °C for 2 h. This layer prevents contact of spheroids with the plastic of the well. Growth medium was partially removed from previously formed spheroid and each spheroid was picked up and pipetted in a small drop of collagen 1 (100 µL), previously dispensed on the bottom of a petri dish, with/without half of the needed Pirfenidone concentration. This procedure was applied to allow a better inclusion of the spheroid in the matrix. After 15 min, each spheroid was moved onto each collagen-coated 96 flat-bottom wells. Following 30 min-incubation 50 µL of complete medium with/without

half concentration of Pirfenidone were added. Final concentration of Pirfenidone was therefore 300 µg/mL. Plates were then incubated at 37 °C in a CO_2 incubator and evaluation of the invasion area was determined at different time points (24, 36, 48, 72, 132 h). The area dimensions were calculated by subtracting the inner core-spheroid area (ICA) from the total area covered by invading cells (outer cell borders, OCB) and the spheroid itself, obtaining the derived growth area (OCB-ICA). The calculated (OCB-ICA)/OCB ratio was then used to express the percentage of the area occupied by growing cells.

2.10 Statistical Analysis

Whenever indicated, Student-*t* test and the Bonferroni's correction were applied to evaluate the statistical significance; *: $0.01 < p \leq 0.05$; **: $0.001 < p \leq 0.01$; ***: $p \leq 0.001$.

3. Results

3.1 Patients' Clinical and Diagnostic features.

Clinical details of the patients employed in the present study are reported in **Supplementary Tables 1**,**2**. For research purposes, we received the bronchoalveolar lavage of 43 ILD patients that were out of treatment. These patients were subjected to bronchoscopy and/or to criobiopsy for diagnostic purposes. Based on clinical, histological and cytofluorographic analyses the patients were then diagnosed as IPF (N = 23), fHP (N = 3), CTD-ILD (N = 5), IPAF (N = 4), NSIP (N = 3), Sarcoidosis (N = 3) and IgG-related disease (IgG4-RD, N = 2) (see **Supplementary Tables 1,2**).

3.2 Derivation, Expansion and Morphological Evaluation of Fibroblasts From ILD Patients

Fibroblasts were derived from the BAL fluids of ILD patients. In a number of cases the cells could be expanded only for a short time, while in a few cases we could grow the cells for a longer time and for numerous passages (usually 10–12 or 36 in a unique case). Briefly, cells of the BAL fluid were first pelleted by centrifugation and then seeded in a 24-well plate in complete culture medium, adding a sub-optimal concentration of FGF2 the next day. In some cases, after 8–10 days, a few fibroblasts started to grow and to form colonies: fibroblasts reaching confluence were then detached and in part processed for RNA studies. When possible, the remaining cells were re-seeded and expanded in 24 or 6-well plates. Through this procedure we could derive a small number of cells from 20 ILD BAL fluids, out of 43 received (46%). Among these 20 samples we could further derive a larger quantity of cells from 11 patients (25%; 3 IPF, 2 fHP, 1 Sarcoidosis, 3 IPAF, 1 CTD-ILD and 1 NSIP) (**Supplementary Table 1**). Morphological features of fibroblasts derived from some ILD patients, as compared to the control cell line MRC5, are shown in Fig. 1A. Fibroblasts derived from one IPF patient, as well as those from two fibrotic HP patients, appear flattened and enlarged with a polygonal aspect, as compared with fibroblasts derived from patients with NSIP, IPAF, CTD-ILD, or either the control cell line MRC5, that are more spindle shaped. These observations highlight that fibroblasts derived from different ILD patients may show a certain heterogeneity, possibly related to higher levels of fibrosis observed in IPF or in fHP, than in the others (see **Supplementary Table 1**). This evidence could further support the suggestion that these fibroblasts might be truly representative of the ongoing fibrotic process. Fig. 1B,C further display the expression of β-galactosidase (β-gal), a marker of senescence, in fibroblasts derived from one IPF case (#17) versus the control cell line MRC5 at the same passage (p5). A significant higher number of β-gal positive cells were found for fibroblasts derived from the IPF patient, as compared to the control cell line: indeed there is a general consensus that fibroblast senescence is increased and persistent in lungs of IPF patients and that it is linked to the pathogenesis of the disease [17].

3.3 Analysis of the Expression of Typical Markers of Fibroblasts/Myofibroblasts by Quantitative RT-PCR and Cytofluorographic Analyses

From the RNA of fibroblasts derived from 19 patients, we further examined, by quantitative RT-PCR, the expression of specific markers, such as α-SMA, type 1 collagen and Fibronectin EDA and EDB, which are usually upregulated during the differentiation of fibroblasts toward myofibroblast. As shown in Fig. 2 the expression of Type I Collagen, α-SMA and fibronectin resulted higher in ILD-fibroblasts than in fibroblasts derived from normal controls, although without reaching statistical significant. The expression of the FGF2 receptor (FGF2R) also appeared higher in fibroblasts from ILD than in those from controls (Fig. 2).

Cytofluorographic analyses of fibroblasts derived from representative ILD patients have further shown that typical markers of mesenchymal/fibroblast cells were expressed in all the derived fibroblasts such as CD105, CD90 and CD73 (**Supplementary Fig. 1**). These fibroblasts were also positive for vimentin but negative for CD45 (data not shown), thus confirming that they are of mesenchymal and not of hematopoietic origin, such as fibrocytes. We further observed that ILD-fibroblasts display a higher expression of α-SMA and type I Collagen than the control cell line MRC5 (Fig. 2B), in agreement with their differentiation towards myofibroblasts, typically involved in pulmonary fibrosis.

3.4 Evaluation of Proliferation and Cytotoxic Activity of Pirfenidone in Fibroblasts Cultured in 2D Models

We next evaluated proliferative response of ILD-fibroblasts to FGF, TGFβ or TGFβ + Pirfenidone. As shown in Fig. 3A, FGF weakly stimulated proliferation of fibroblasts derived from the different patients. Pirfenidone was capable of inhibiting TGFβ-induced prolif-

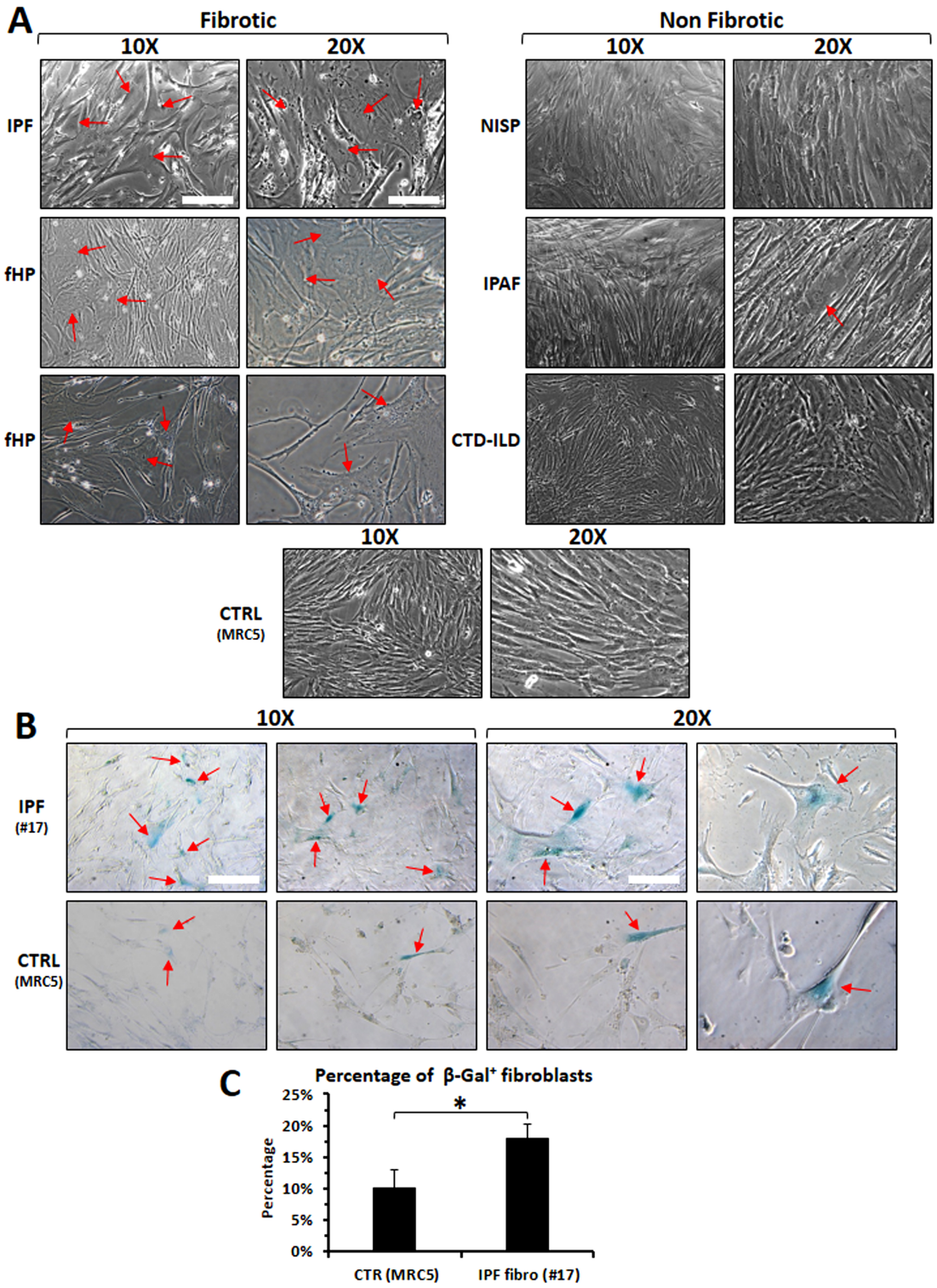

Fig. 1. Differences in morphological features or level-senescence among fibroblasts derived from various ILD patients (fibrotic *vs* non-fibrotic) or in comparison with the control cell line MRC5. (A) Morphological representation of fibroblasts derived from different ILD patients versus fibroblasts derived from a healthy lung-fibroblast cell line. Red arrows indicate cells with enlarged and flattened shapes, typical of myofibroblast differentiation. (B) a higher number of cells positive for β-galactosidase (red arrows) were observed in fibroblasts derived from one IPF patient than in control fibroblasts (MRC5). (C) Histograms depict the mean $\pm$ SD of B-gal positive cell of 5 images for each sample. IPF, Interstitial Pulmonary Fibrosis; fHP, fibrotic Hypersensitivity Pneumonitis; NISP, Non-Specific Interstitial Pneumonia; IPAF, Interstitial Pneumonia with Autoimmune Features; CTD-ILD, Connective Tissue Disease-Interstitial Lung Disease. White Bars correspond to 12.5 µm and 25 µm for 10$\times$ and 20$\times$ images, respectively; *: $0.01 < p \leq 0.05$.

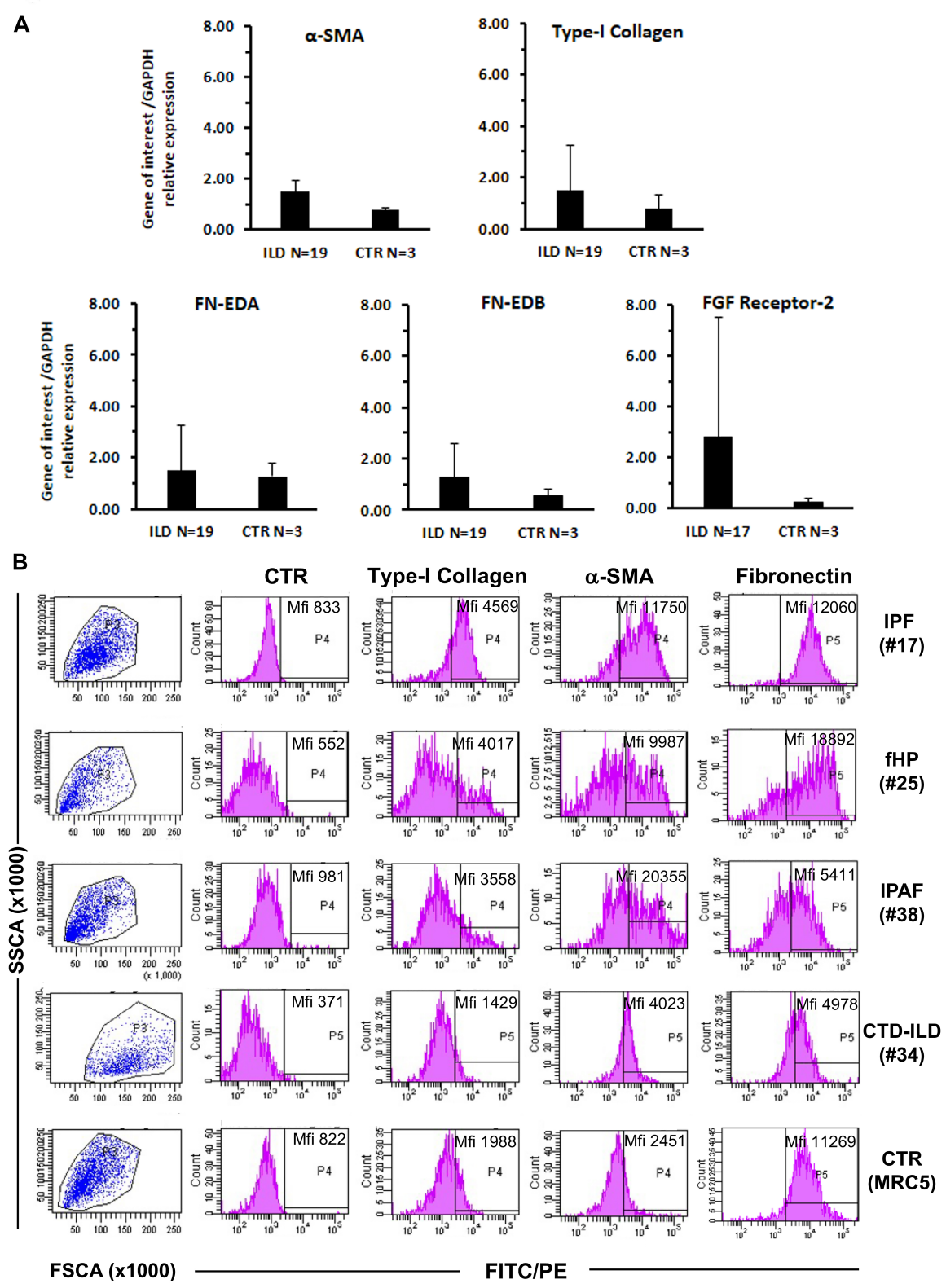

Fig. 2. Quantitative RT-PCR determination and cytofluorographic analysis of typical markers of fibroblast/myofibroblast differentiation in cells derived from ILD patients versus controls. (A) mRNA expression of alpha-SMA, collagen type-I, fibronectin and FGF2 receptor was higher in fibroblasts from ILD patients than in fibroblasts from controls (CTR). (B) Mean Fluorescence Intensity (Mfi) of α-SMA, collagen-I and, to a lesser extent Fibronectin, was higher in fibroblasts from ILD-patients than in the control cell line MRC5. Numbers in parenthesis relate to the ID number of representative cases of different types of ILD. FGF, Fibroblast growth factor 2; α-SMA, alpha Smooth Muscle Actin.

eration (Fig. 3B–E) with an inhibition range of 20–32% when Pirfenidone was used at 150 µg/mL. The response to pirfenidone displayed, however, a dose-dependent mode, particularly evident for fibroblasts from the fHP (#25) and CTD-ILD (#34) cases, reaching almost 50% of inhibition (Fig. 4A). On the contrary fibroblasts of the NSIP case (#41) were almost unresponsive and a partial inhibition (23%) was observed at the highest concentration of 450 µg/mL. The clear dose-response effect exerted by Pirfenidone is evident in the representative images of Fig. 4B referred to ILD patient #34. Moreover, the treatment with Pirfenidone down-modulated the TGFβ-induced expression of actin fibers in fibroblasts derived from two ILD patients (#25, #34), as depicted in Fig. 5.

3.5 Inhibition of Migration by Pirfenidone

The effect of pirfenidone on migration of ILD-fibroblasts was further evaluated by the use of a wound scratch assay [18] thus measuring fibroblasts polarizing and migrating in the wound space, with and without Pirfenidone treatment. Fig. 6A shows the migration of fibroblasts from one representative case of 5 tested following the stimulation with TGFβ (5 ng/mL) with/without Pirfenidone treatment (150 µg/mL), at different time-points (Fig. 6A). As shown in Fig. 6 Pirfenidone inhibited the ability of fibroblasts derived from different ILD-patients (#17, #25, #34, #38 and #41) to migrate across the lesion borders.

3.6 Assessment of Growth and Cytotoxic Activity of Pirfenidone in a 3D Model of Culture of ILD- Fibroblasts

We next assessed the cytotoxic response to Pirfenidone of ILD-fibroblasts in 3D cultures. We took advantage of ultra-low attachment 96 U-bottom well plates to establish spheroids (only ILD-fibroblasts) or organoids (epithelial or endothelial cells + ILD-fibroblasts) and to further determine the activity of Pirfenidone. Fig. 7A,B shows that the formation of spheroids of ILD-fibroblasts was inhibited after Pirfenidone treatment (300 µg/mL) for 72 h with the exception of fibroblasts derived from one NSIP case (#41). A range of inhibition of 32% was detected among the responsive cases, with a more evident inhibition value for fibroblasts derived from the IPF case #17 (65%). Pirfenidone was also active in spheroids established with the epithelial adenocarcinoma A549 cells (41% of inhibition) but not with the endothelial cell line HECV (Fig. 7A,B). We then determined Pirfenidone cytotoxicity in a model of organoids composed of fibroblasts and A549 or HECV cells together: Pirfenidone inhibited the growth of A549+fibroblasts organoids (mean of 3 different added fibroblasts tested: 40% of inhibition), while a very weak effect was detectable for organoids formed by the endothelial HECV cells plus ILD-fibroblasts (Fig. 7C,D). It can be of further interest to note that the response behavior of the cells cultured in 2D was similar to cells cultured in 3D models (**Supplementary Fig. 2**). Ineffectiveness of the pirfenidone treatment on fibroblasts from the NSIP patient #41 was also confirmed, although a weak anti-proliferative effect (23%) was detectable when Pirfenidone was added at the concentration of 450 µg/mL and fibroblasts were tested in the 2 model, as described before.

3.7 Determination of Fibroblasts-invasiveness in a 3D Model

Spheroids derived as above described were further tested for cell invasiveness. We evaluated the migratory mobility of the cells by determining the enlargement of the area of fibroblast migration with time and treatment as a percentage of the total occupied area (Fig. 8; see also **Supplementary Fig. 3**). Cell spreading, well evident already from 36–48 h, was significantly reduced by Pirfenidone treatment, as depicted in Fig. 8A,B, particularly in fibroblasts derived from the one CTD-ILD case tested (#34).

4. Discussion

Different to surgical lung biopsy BAL is a minimally invasive procedure. In clinical practice its application represents a valuable tool to refine the differential diagnosis of ILD, through the determination of the immune cell counts [19]. Since BAL provides direct access to the alveolar and bronchial epithelium, as well as to the surrounding microenvironment, studies on its composition, both in terms of soluble factors or either cells, might shed new light on the multiple pathogenetic processes taking place in progressive pulmonary fibrosis. The culture and expansion of cells involved in pulmonary fibrosis can be therefore useful to exploit novel *in vitro* models to better define the complex interactions among different lung cell subtypes and even for personalized medicine to assess responses to specific therapies [20]. We have described here the possibility of deriving fibroblasts/myofibroblasts from the BAL of various ILD patients. Although it is clear that the cells recovery from tissue biopsy is certainly easier and more productive than from BAL fluids, we would like to highlight that the culture-protocol that we have described appears quite feasible. Apart from potential handling contaminations, which could be reduced by the concomitant addition of a proper antibiotic mix to the lavage fluid samples, the procedures are simple, cost-effective and devoid of any ethical concerns.

Looking at morphological and immunophenotypic features of fibroblasts derived from ILD-patients, versus normal controls, we could observe that those derived from ILD-patients showed typical characteristics of differentiation toward myofibroblasts, such as higher collagen I or α-SMA expression. In addition, in fibroblasts from a IPF patients there was also a tendency to express higher levels of β-galactosidase as a sign of senescence: there is indeed a close link between cellular senescence and IPF [21].

The expression of the FGF2 receptor was also higher in fibroblasts derived from ILD patients than in those from

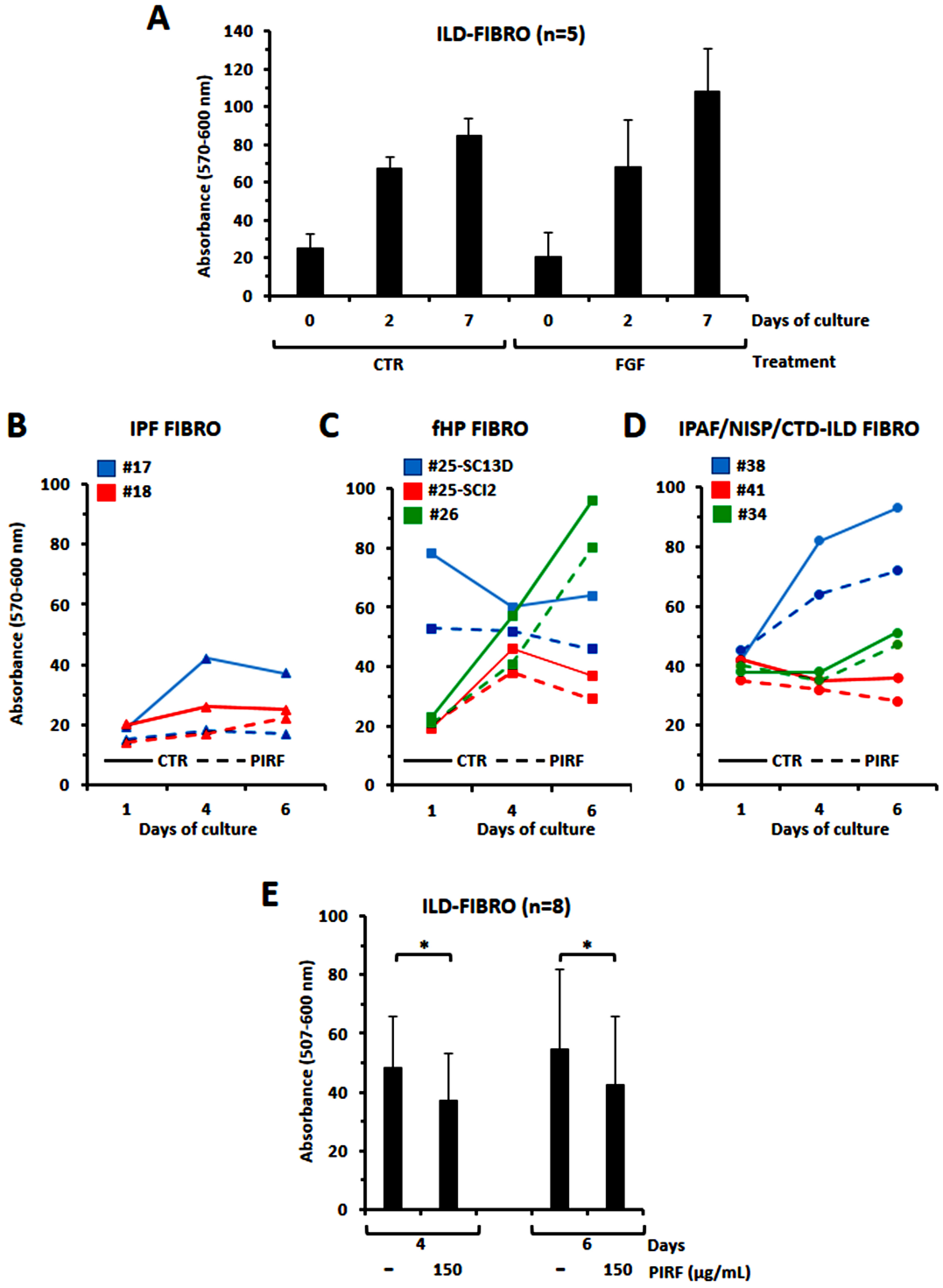

Fig. 3. Evaluation of the proliferative response to FGF2 or to TGFβ or TGFβ+Pirfenidone in fibroblasts derived from different ILD patients. (A) FGF2 induced a weak stimulation of the proliferation. (B–D) Proliferation of ILD-fibroblasts induced by TGFβ resulted inhibited by the addition of Pirfenidone (PIRF) at a concentration of 150 µg/mL. For each graph the depicted number refers to patients' ID from which the fibroblasts were derived (**Supplementary Table 1**). SCI13D and SCI2 were derived from two BALs of the same patient (#25), received at different times. (E) Histograms represent the summary of the single cases presented in panel (B–D), further confirming that, as a whole, the inhibitory effect exerted by Pirfenidone was significant after 4 as well as after 6 days of treatment. *: $0.01 < p \leq 0.05$.

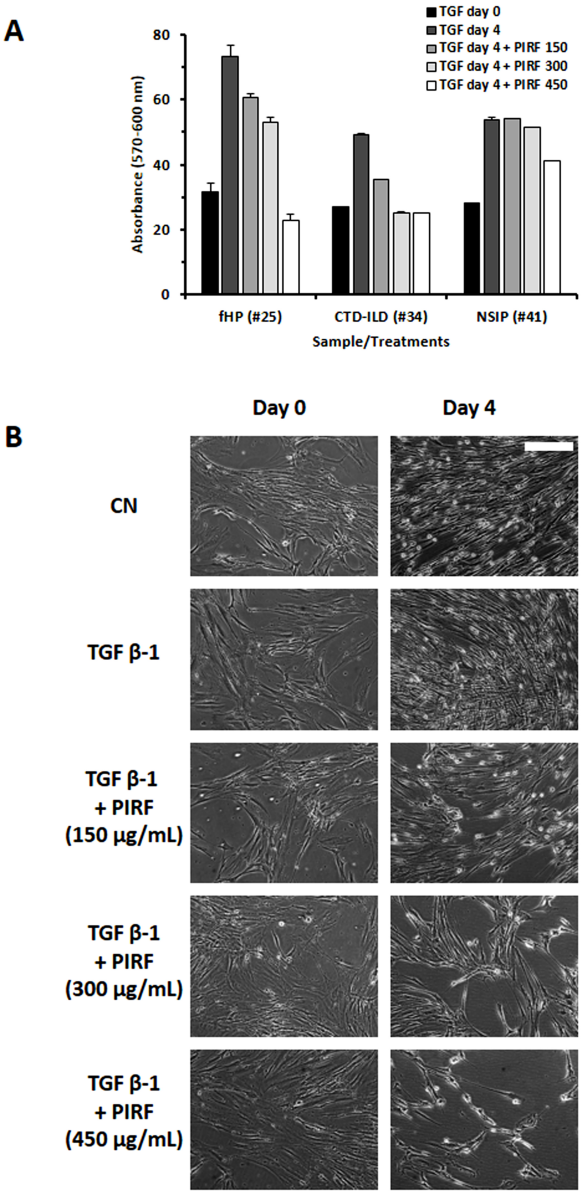

Fig. 4. Determination of dose-dependency effect of Pirfenidone. (A) Evaluation of the growth of fibroblasts derived from 3 different ILD patients treated with increasing doses of Pirfenidone (150, 300 and 400 µg/mL). Histograms represent the mean ± SD of the 3 cases (fHP #25; CTD-ILD #34; NSIP #41) each assessed in duplicate. (B) Images represent cultures of fibroblasts derived from one representative patient (#34) exposed to different concentrations of Pirfenidone. The white bar corresponds to 12.5 µm.

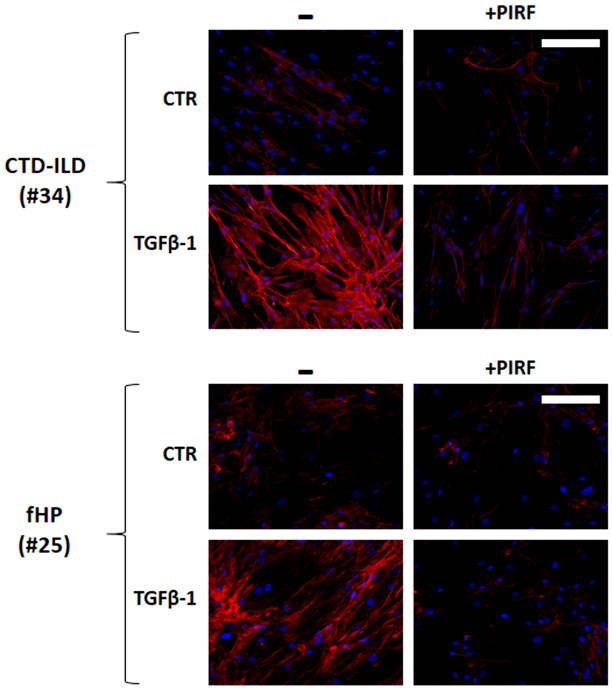

Fig. 5. Evaluation of F-actin expression in fibroblasts derived from two Pirfenidone-treated or -untreated ILD patients. Pirfenidone consistently reduced the expression of F-actin fiber fluorescence in fibroblasts derived from two ILD patients with/without TGFβ stimulation. The white bar corresponds to 25 µm.

normal controls, and we could also demonstrate a slight proliferation to FGF2. Indeed, in our protocol we used to add a sub-optimal concentration of FGF2 to the cultures to better expand fibroblasts. However, conflicting results have been reported about the role of FGF2 in driving fibroblasts to myofibroblasts differentiation, as well as in the progression of the fibrotic process [22–26]. Apparently FGF2 induces fibroblast dedifferentiation, with subsequent reduction of collagen and ECM production, but, at the same time, stimulates their proliferation. We have, however, previously demonstrated that, after FGF2 treatment, the observed down-modulation of collagen I and α-SMA expression, in fibroblasts derived from a fHP patient, was only a transient phenomenon [2]. As previously reported, FGF2 may indeed favor the expansion of mesenchymal cells by providing a reservoir of less differentiated and proliferating cells [27]. Altogether our data suggests that FGF2 appears useful in expanding fibroblasts/myofibroblasts in *in vitro* cultures. Further investigations, however, will better clarify whether FGF2 is pro-fibrotic or anti-fibrotic or whether a complex microenvironmental context, such as the concomitant presence of particular cytokines, could also influence its activity.

Currently two antifibrotic drugs, Nintedanib and Pirfenidone are approved for the treatment of IPF. While the use of Nintedanib has recently been approved also for non-IPF fibrotic ILD, the efficacy of Pirfenidone in these patients is still debated and needs to be fully established [28]. Nintedanib is a receptor tyrosine kinase inhibitor of platelet-derived growth factor receptor (PDGFR)-, vascular endothelial growth factor receptor (VEGFR)- and fibroblast growth factor receptor (FGFR), that critically regulate myofibroblast transformation and collagen production under

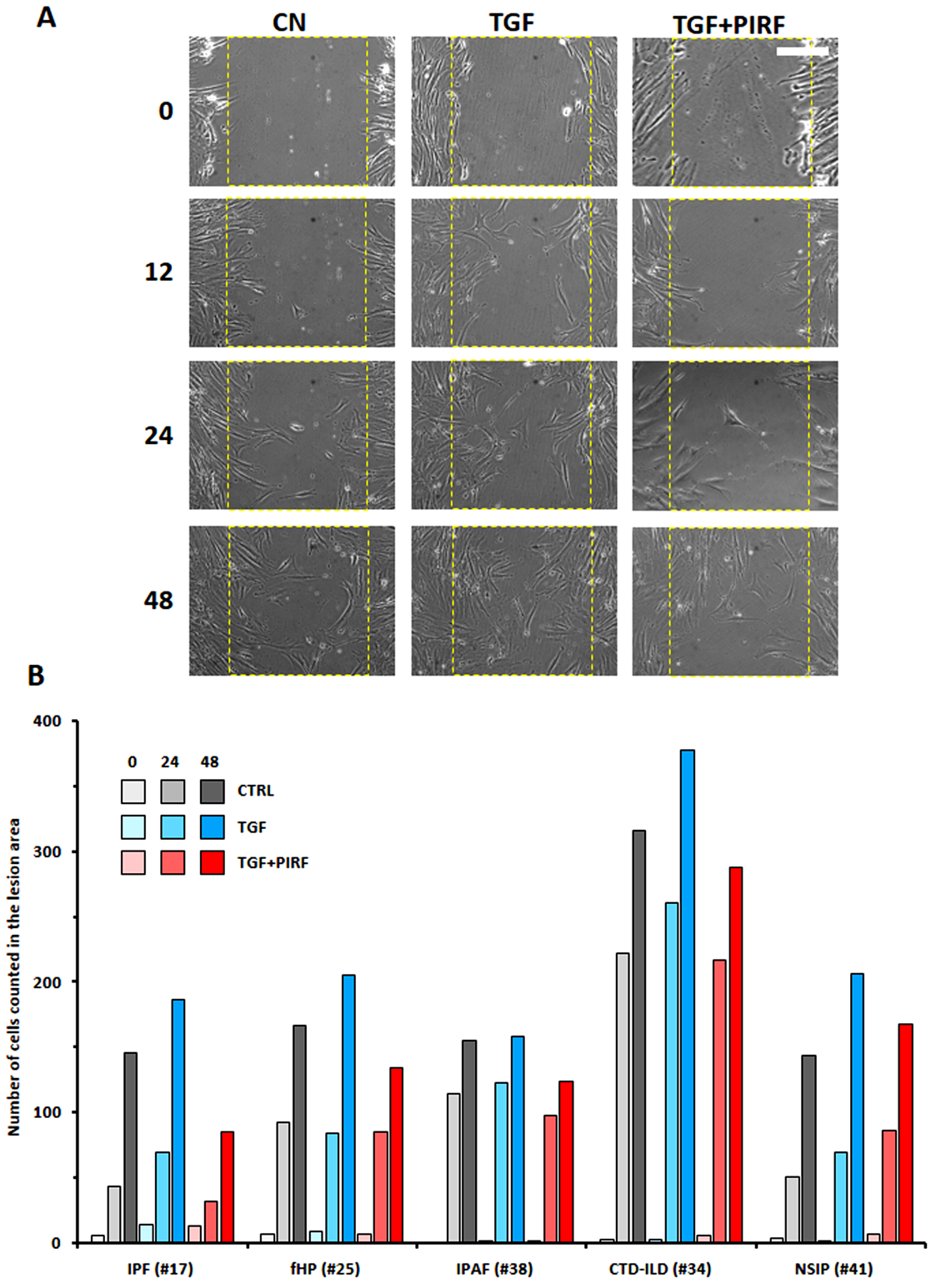

Fig. 6. Determination of the migratory capacity of ILD-fibroblasts in a 2D system through a wound scratch test assay. (A) The migratory capacity of ILD-fibroblasts induced by TGFβ, treated or untreated with Pirfenidone, was determined by acquiring images of the cells filling-in the lesion gap (yellow lines) at the indicated time points (0, 12, 24 and 48 h), as here shown for fibroblasts from one representative patient (#17). (B) Histograms represent the counted cells within the lesion's boundaries for fibroblasts derived from ILD-patients at several time-points and under different treatments. Experiments were performed in duplicate for each time point and treatments and the values are the mean of two separate experiments. The white bar corresponds to 12.5 µm.

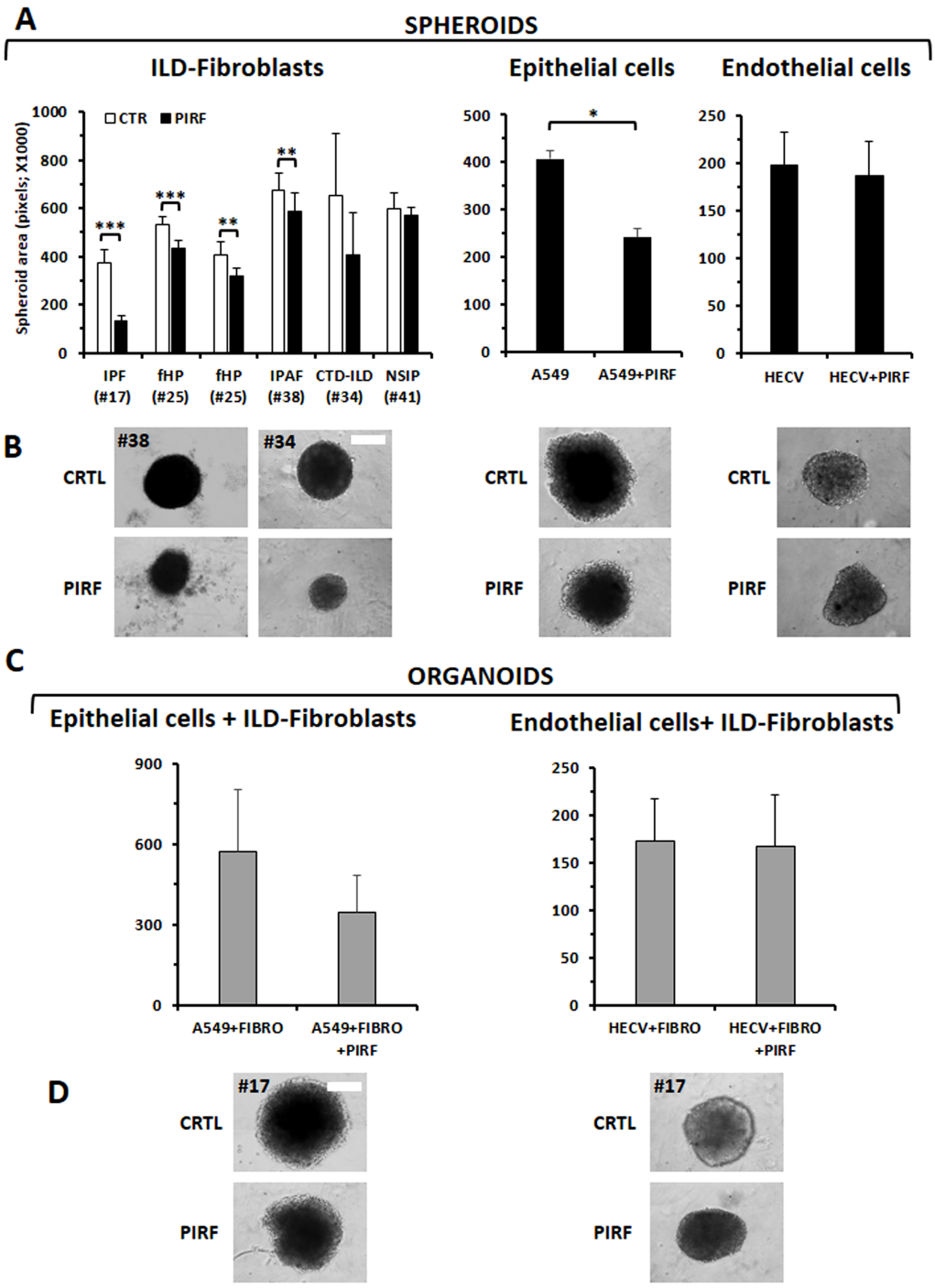

Fig. 7. Evaluation of the Pirfenidone activity on ILD-fibroblasts, or epithelial (A549) or endothelial (HECV) cells, in a 3D model of *in vitro* growth. (A) Spheroids composed of fibroblasts derived from different ILD patients, or A549 or HECV cell lines, were tested with Pirfenidone (300 µg/mL): pirfenidone significantly inhibited proliferation of ILD-fibroblasts with the exception of the NSIP case. The epithelial cell line A549 resulted inhibited but not the endothelial cell line HECV. (B) Images depict representative spheroids for each sample type. The white bar corresponds to 25 µm. (C) Organoids composed by A549 or HECV cells and ILD-fibroblasts were treated with pirfenidone (300 µg/mL): the drug resulted effective as a trend, although without statistical significance, for A549 cells+ILD-fibroblasts (3 cases assessed) but not for HECV cells+ILD-fibroblasts (2 cases assessed). Histograms values are the mean ± SD of 6 spheroids-areas or organoids-area per condition, evaluated as indicated in the methods section. (D) Images display representative organoids for each sample type. The white bar corresponds to 25 µm; *: $0.01 < p \leq 0.05$; **: $0.001 < p \leq 0.01$. ***: $p \leq 0.001$.

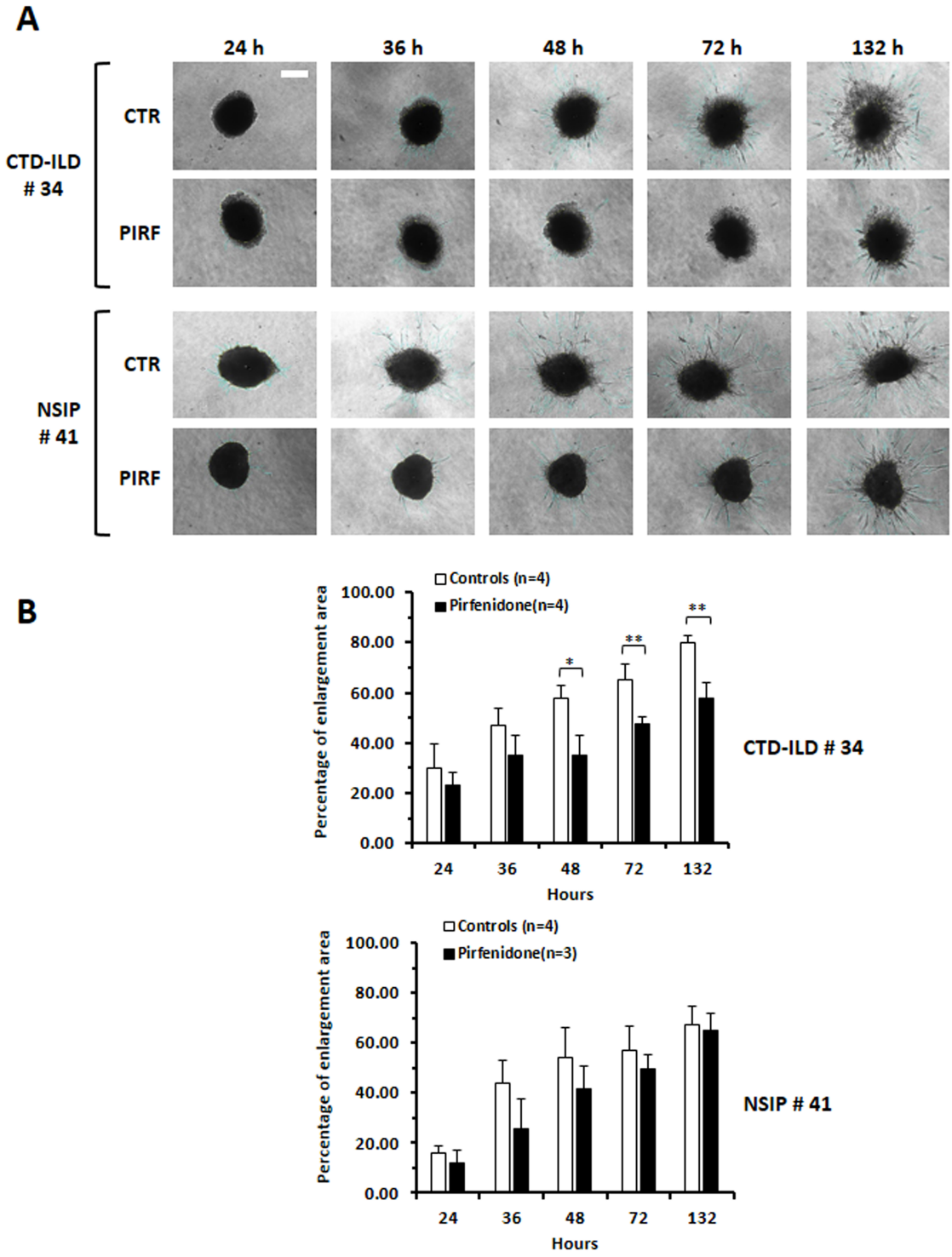

Fig. 8. Evaluation of the efficacy of Pirfenidone treatment on invasiveness of ILD-fibroblasts grown in 3D. (A) The invasiveness of ILD-fibroblasts composing the spheroids resulted inhibited following pirfenidone treatment (300 ug/mL) at different time points (24, 36, 48, 72 and 132 h). Images are representative of fibroblasts from two ILD patients. The white bar corresponds to 25 µm. (B) Histograms depict the mean $\pm$ SD of the percentage of enlargement area of different spheroids (N is indicated in each graph) per each treatment/time point, and refer to the two different ILD cases tested (#34 and #41); *: $0.01 < p \leq 0.05$; **: $0.001 < p \leq 0.01$.

fibrotic conditions [29]. The direct targets of Pirfenidone are still unknown, however it has been previously demonstrated that its anti-fibrotic property depends on the inhibition of production of various pro-fibrotic cytokines and growth factors, such as TGF-β1, basic-FGF, PDGF, Interleukin 1β (IL-1β), or TNFα [30].

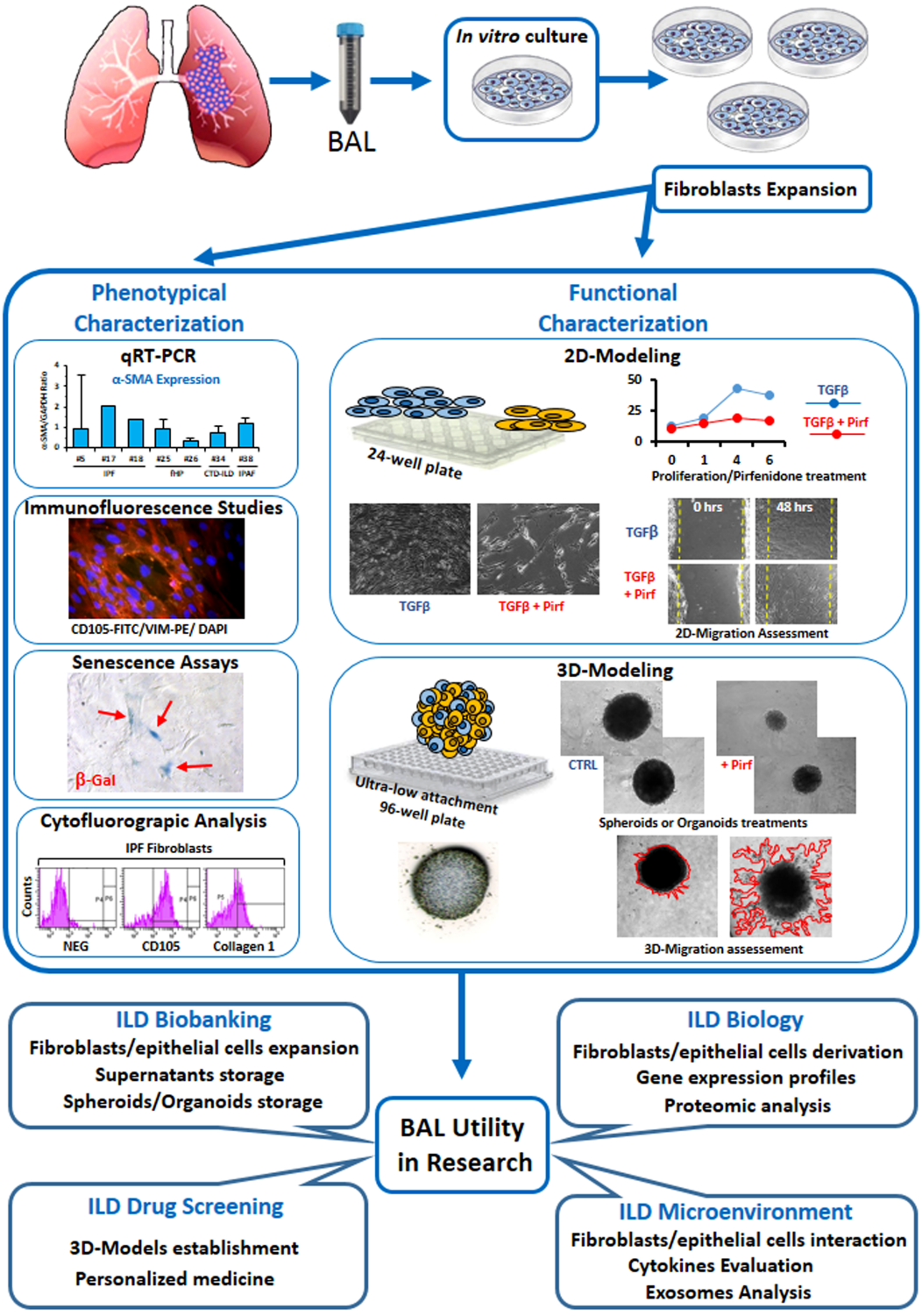

Fig. 9. Representation of the utility of bronchoalveolar lavage in research. Summary of the different passages used to derive fibroblasts from the bronchoalveolar lavage of ILD-patients and to characterize them phenotypically and functionally. The present figure was created using freely available cartoons and personal unpublished data using Microsoft Power Point software.

By assessing the activity of Pirfenidone on proliferation and migration of fibroblasts/myofibroblasts derived from different ILD-patients we detected a discrete inhibition for those from IPF patients as well as for those from non-IPF ILD, except for one case diagnosed as NSIP, not presenting pulmonary fibrosis (#41). The effectiveness of

Pirfenidone was dose-dependent, and resulted particularly evident at the dose of 300–450 µg/mL, in line with previous studies [31]. NSIP-derived fibroblasts (patient #41), still unresponsive at the dose of 300 µg/mL, started to show a response, albeit weak (23%), when treated with 450 µg/mL of Pirfenidone. The observation that these fibroblasts appear more resistant to Pirfenidone treatment might reflect differences in their phenotype. Potential discriminative features among fibroblasts derived from IPF and NSIP patients have been addressed in a few previous studies. Miki H. and coauthors [32] reported a greater contractility of fibroblasts derived from lung biopsy of IPF/UIP than NSIP patients: this feature appeared in relation with a higher Fibronectin (FN-EDA) content. Barbara Orzechowska and collaborators [33], further exploring the impact of substrate elasticity on the properties of cell lines derived from IPF, NSIP or a healthy subject, demonstrated that fibroblasts derived from the two disorders can be discriminated on the basis of their physical and chemical properties. Gene expression profiling of explanted lung from patients with IPF or NSIP further highlighted that in the latter the genes enriched were related to immune reactions, such as T cell response or leukocytes recruitment to the lung, while in IPF they were related to senescence, myofibroblasts differentiation and collagen deposition [34]. Of note, the BAL of patient #41 was characterized by a very high percentage of lymphocytes and a low number of monocytes/macrophages, different to most of the other cases (**Supplementary Table 1**), further suggesting a possible link to autoimmune reaction.

We have further demonstrated that Pirfenidone reduced the expression of F-actin stress fiber in fibroblasts derived from various ILD [2]. The multiple effects of Pirfenidone were clearly evident on cells cultured as monolayers, but also on spheroids or organoids, which possibly better mimick the lung tissue 3D *in vitro*. Since the same trends and effects were displayed among the exact same types of ILD both in the monolayers and in the spheroid/organoid cultures (**Supplementary Fig. 2**), these close mirroring results, between 2D- and 3D-culture systems, may suggest that those micromass cultures, requiring a much lower number of cells, could easily substitute larger, longer and possibly more demanding traditional monolayer-based approaches. Although the number of samples that we have tested here is too low, thus deserving to be better explored, these data may suggest the potential translational nature of these models, especially the more physiological 3D one, for preclinical and personalized drug screening.

A limiting point of the present study might however be the missing proof that ILD-derived fibroblasts really represent those involved in the fibrotic process. Although we cannot state that the BAL derived fibroblasts are directly representative of the ones expanded during fibrosis, or either located within the fibroblastic foci, it might be conceivable to assume that a larger number of fibroblasts may be present in BAL from patients with progressive fibrosis. Therefore, it appears mandatory to characterize ILD-derived fibroblasts, after their expansion, for the expression of typical myofibrotic markers. In addition, in support of a putative correspondence between fibroblasts infiltrating the lung parenchima and those derived from the BAL fluid, was the evidence that a trisomy 10, exhibited as a peculiar feature by fibroblasts (SCI13D) obtained from an fHP patients (#25), was also found in fibroblasts infiltrating the lung tissue of the cryobioptic specimen, as we previously described [2]. Only a limited number of studies have to date compared fibroblasts isolated from BAL fluids with those derived from tissue, probably due to the difficulty of obtaining BAL and bioptic-tissue from the same patients. In the future further studies might bridge this gap: more sophisticated techniques, matching the two sample sources and coupled to omics-analysis, could clarify the respective origin, intrinsic nature and derivation of those fibroblasts. It is, however, also true that a certain heterogeneity may be present among fibroblasts involved in fibrosis, possibly related to their mesenchymal origin and their plasticity [35].

We are aware that, although representative of the composite family of ILD disease, data samples described here remain limited and need to be implemented to provide sufficient ground for possible discrimination among the different ILD subtypes. Moreover, our 3D organotypic coculture system represents just an early step in lung modeling, reflecting more cell-to-cell interaction rather than fully mimicking tissue structure, suggesting however that it is nonetheless worth of future exploration and deeper understanding.

5. Conclusion

Collectively the data described here, as well as those previously reported from other Authors [36,37], have demonstrated that recovering ILD-BAL fluids represents a valuable and useful tool not only for diagnostic purposes but also for a variety of research investigations. As summarized in our experimental scheme described in Fig. 9, ILD-BAL, other than providing a potential source of cells, such as fibroblasts/myofibroblasts, fibrocytes or even epithelial cells, it may also reveal cytokines/growth factors potentially involved in the fibrotic process. Clarification of the role played by exosomes present within the BAL, with their cargo, has recently further emerged as a novel manner to study the intimate cross-talk among different cell subpopulations of the lung, as well as to identify biomarkers potentially discriminating different ILD [38]. In addition, since IPF patients show a susceptibility developing lung cancer, these studies might also reveal their relationships. To this regard it has been for example reported that exosomes released by IPF-senescent fibroblasts influence tumor progression by activating the PI3K-AKT-mTOR pathway [39]. Based on the overall data described above, we therefore suggest that the use of a small volume of BAL and its biobanking, as a source of cells and soluble factors from

a large number of ILD-patients, can be taken into great consideration to develop *in vitro* models of pulmonary fibrosis, trying to reveal novel insights in the pathogenetic process.

Availability of Data and Materials

Data supporting the findings of this study are available from the corresponding author upon reasonable request.

Author Contributions

Conceptualization, writing and editing: DdT, PG; Clinical assessment: EB, MG, FC and FM; Lab experiments: DdT, PG, MB, PA; Supervisioning: DdT, MG, EB, FM, FC. All authors have read and agreed with the final version of the manuscript. All authors have participated sufficiently in the work to take public responbility for appropriate portions of the content and agreed to be accountable for all aspects of the work in ensuring that questions related to its accuracy or integrity. All authors contributed to editorial changes in the manuscript.

Ethics Approval and Consent to Participate

This study was conducted according to the guidelines of the Declaration of Helsinki; all procedures were also performed according to the standard Good Clinical Practices, following the national current rules and regulations, and the study was approved by the Institutional Ethics Committee of the IRCCS Ospedale Policlinico San Martino, Genova, Italy (protocol code ILDFIBRO020, n. of Register CER Liguria: 523/2020 DB id 10931). Within the study, all biological samples were anonymized prior to processing. Written informed consent was obtained from all participants involved in the study.

Acknowledgment

Not applicable.

Funding

5X1000 2022 C809A (E.B.); Italian Ministry of Health (Ricerca Corrente 2022-2024).

Conflict of Interest

The authors declare no conflict of interest.

Supplementary Material

Supplementary material associated with this article can be found, in the online version, at https://doi.org/10.31083/FBL38726.

References

[1] Adams TS, Schupp JC, Poli S, Ayaub EA, Neumark N, Ahangari F, *et al*. Single-cell RNA-seq reveals ectopic and aberrant lung-resident cell populations in idiopathic pulmonary fibrosis. Science Advances. 2020; 6: eaba1983. https://doi.org/10.1126/sciadv.aba1983.

[2] Giannoni P, Grosso M, Fugazza G, Nizzari M, Capra MC, Bianchi R, *et al*. Establishment and Characterization of a Novel Fibroblastic Cell Line (SCI13D) Derived from the Broncho-Alveolar Lavage of a Patient with Fibrotic Hypersensitivity Pneumonitis. Biomedicines. 2021; 9: 1193. https://doi.org/10.3390/biomedicines9091193.

[3] Wijsenbeek M, Kreuter M, Olson A, Fischer A, Bendstrup E, Wells CD, *et al*. Progressive fibrosing interstitial lung diseases: current practice in diagnosis and management. Current Medical Research and Opinion. 2019; 35: 2015–2024. https://doi.org/10.1080/03007995.2019.1647040.

[4] Gibson CD, Kugler MC, Deshwal H, Munger JS, Condos R. Advances in Targeted Therapy for Progressive Fibrosing Interstitial Lung Disease. Lung. 2020; 198: 597–608. https://doi.org/10.1007/s00408-020-00370-1.

[5] Selman M, Pardo A. When things go wrong: exploring possible mechanisms driving the progressive fibrosis phenotype in interstitial lung diseases. The European Respiratory Journal. 2021; 58: 2004507. https://doi.org/10.1183/13993003.04507-2020.

[6] Sindhu A, Jadhav U, Ghewade B, Wagh P, Yadav P. Unveiling the Diagnostic Potential: A Comprehensive Review of Bronchoalveolar Lavage in Interstitial Lung Disease. Cureus. 2024; 16: e52793. https://doi.org/10.7759/cureus.52793.

[7] Samarelli AV, Masciale V, Aramini B, Coló GP, Tonelli R, Marchioni A, *et al*. Molecular Mechanisms and Cellular Contribution from Lung Fibrosis to Lung Cancer Development. International Journal of Molecular Sciences. 2021; 22: 12179. https://doi.org/10.3390/ijms222212179.

[8] Wolters PJ, Collard HR, Jones KD. Pathogenesis of idiopathic pulmonary fibrosis. Annual Review of Pathology. 2014; 9: 157–179. https://doi.org/10.1146/annurev-pathol-012513-104706.

[9] Lama VN, Phan SH. The extrapulmonary origin of fibroblasts: stem/progenitor cells and beyond. Proceedings of the American Thoracic Society. 2006; 3: 373–376. https://doi.org/10.1513/pats.200512-133TK.

[10] Lynch MD, Watt FM. Fibroblast heterogeneity: implications for human disease. The Journal of Clinical Investigation. 2018; 128: 26–35. https://doi.org/10.1172/JCI93555.

[11] Moeller A, Gilpin SE, Ask K, Cox G, Cook D, Gauldie J, *et al*. Circulating fibrocytes are an indicator of poor prognosis in idiopathic pulmonary fibrosis. American Journal of Respiratory and Critical Care Medicine. 2009; 179: 588–594. https://doi.org/10.1164/rccm.200810-1534OC.

[12] Raghu G, Remy-Jardin M, Myers JL, Richeldi L, Ryerson CJ, Lederer DJ, *et al*. Diagnosis of Idiopathic Pulmonary Fibrosis. An Official ATS/ERS/JRS/ALAT Clinical Practice Guideline. American Journal of Respiratory and Critical Care Medicine. 2018; 198: e44–e68. https://doi.org/10.1164/rccm.201807-1255ST.

[13] Raghu G, Remy-Jardin M, Richeldi L, Thomson CC, Inoue Y, Johkoh T, *et al*. Idiopathic Pulmonary Fibrosis (an Update) and Progressive Pulmonary Fibrosis in Adults: An Official ATS/ERS/JRS/ALAT Clinical Practice Guideline. American Journal of Respiratory and Critical Care Medicine. 2022; 205: e18–e47. https://doi.org/10.1164/rccm.202202-0399ST.

[14] Barisione E, Salio M, Romagnoli M, Praticò A, Bargagli E, Corbetta L. Competence in transbronchial cryobiopsy. Panminerva Medica. 2019; 61: 290–297. https://doi.org/10.23736/S0031-0808.18.03567-X.

[15] Shapiro DL, Nardone LL, Rooney SA, Motoyama EK, Munoz JL. Phospholipid biosynthesis and secretion by a cell line (A549) which resembles type II aleveolar epithelial cells. Biochimica et Biophysica Acta. 1978; 530: 197–207. https://doi.org/10.1016/0005-2760(78)90005-x.

[16] Dsouza KG, Surolia R, Kulkarni T, Li FJ, Singh P, Zeng H, *et al*. Use of a pulmosphere model to evaluate drug antifibrotic re-

sponses in interstitial lung diseases. Respiratory Research. 2023; 24: 96. https://doi.org/10.1186/s12931-023-02404-7.

[17] Álvarez D, Cárdenes N, Sellarés J, Bueno M, Corey C, Hanumanthu VS, *et al*. IPF lung fibroblasts have a senescent phenotype. American Journal of Physiology. Lung Cellular and Molecular Physiology. 2017; 313: L1164–L1173. https://doi.org/10.1152/ajplung.00220.2017.

[18] Cory G. Scratch-wound assay. Methods in Molecular Biology (Clifton, N.J.). 2011; 769: 25–30. https://doi.org/10.1007/978-1-61779-207-6_2.

[19] Chen B, Leng Z, Zhang J, Shi X, Dong S, Wang B. Diagnostic Application of Bronchoalveolar Lavage Fluid Analysis in Cases of Idiopathic Pulmonary Fibrosis in which Diagnosis Cannot Be Confirmed by High-Resolution Computed Tomography. Lung. 2025; 203: 16. https://doi.org/10.1007/s00408-024-00758-3.

[20] Sette G, Lo Cicero S, Blaconà G, Pierandrei S, Bruno SM, Salvati V, *et al*. Theratyping cystic fibrosis *in vitro* in ALI culture and organoid models generated from patient-derived nasal epithelial conditionally reprogrammed stem cells. The European Respiratory Journal. 2021; 58: 2100908. https://doi.org/10.1183/13993003.00908-2021.

[21] Lin Y, Xu Z. Fibroblast Senescence in Idiopathic Pulmonary Fibrosis. Frontiers in Cell and Developmental Biology. 2020; 8: 593283. https://doi.org/10.3389/fcell.2020.593283.

[22] Fortier SM, Penke LR, King D, Pham TX, Ligresti G, Peters-Golden M. Myofibroblast dedifferentiation proceeds via distinct transcriptomic and phenotypic transitions. JCI Insight. 2021; 6: e144799. https://doi.org/10.1172/jci.insight.144799.

[23] Guzy RD, Stoilov I, Elton TJ, Mecham RP, Ornitz DM. Fibroblast growth factor 2 is required for epithelial recovery, but not for pulmonary fibrosis, in response to bleomycin. American Journal of Respiratory Cell and Molecular Biology. 2015; 52: 116–128. https://doi.org/10.1165/rcmb.2014-0184OC.

[24] Koo HY, El-Baz LM, House S, Cilvik SN, Dorry SJ, Shoukry NM, *et al*. Fibroblast growth factor 2 decreases bleomycin-induced pulmonary fibrosis and inhibits fibroblast collagen production and myofibroblast differentiation. The Journal of Pathology. 2018; 246: 54–66. https://doi.org/10.1002/path.5106.

[25] Tian X, Jia Y, Guo Y, Liu H, Cai X, Li Y, *et al*. Fibroblast growth factor 2 acts as an upstream regulator of inhibition of pulmonary fibroblast activation. FEBS Open Bio. 2023; 13: 1895–1909. https://doi.org/10.1002/2211-5463.13691.

[26] Xiao L, Du Y, Shen Y, He Y, Zhao H, Li Z. TGF-beta 1 induced fibroblast proliferation is mediated by the FGF-2/ERK pathway. Frontiers in Bioscience (Landmark Edition). 2012; 17: 2667–2674. https://doi.org/10.2741/4077.

[27] Martin I, Muraglia A, Campanile G, Cancedda R, Quarto R. Fibroblast growth factor-2 supports ex vivo expansion and maintenance of osteogenic precursors from human bone marrow. Endocrinology. 1997; 138: 4456–4462. https://doi.org/10.1210/endo.138.10.5425.

[28] Bellani S, Spagnolo P. What rationale for treatment of occupational interstitial lung diseases with the drugs approved for idiopathic pulmonary fibrosis? Current Opinion in Allergy and Clinical Immunology. 2025; 25: 95–104. https://doi.org/10.1097/ACI.0000000000001055.

[29] Wollin L, Wex E, Pautsch A, Schnapp G, Hostettler KE, Stowasser S, *et al*. Mode of action of nintedanib in the treatment of idiopathic pulmonary fibrosis. The European Respiratory Journal. 2015; 45: 1434–1445. https://doi.org/10.1183/09031936.00174914.

[30] Babariya H, Gaidhane SA, Acharya S, Kumar S. Pirfenidone as a Cornerstone in the Management of Fibrotic Interstitial Lung Diseases and Its Emerging Applications: A Comprehensive Review. Cureus. 2024; 16: e70497. https://doi.org/10.7759/cureus.70497.

[31] Zhang X, Zhang J, Liu Y, Zhu D, Chen D, Zhang Z, *et al*. Pirfenidone inhibits fibroblast proliferation, migration or adhesion and reduces epidural fibrosis in rats via the PI3K/AKT signaling pathway. Biochemical and Biophysical Research Communications. 2021; 547: 183–191. https://doi.org/10.1016/j.bbrc.2021.01.055.

[32] Miki H, Mio T, Nagai S, Hoshino Y, Nagao T, Kitaichi M, *et al*. Fibroblast contractility: usual interstitial pneumonia and nonspecific interstitial pneumonia. American Journal of Respiratory and Critical Care Medicine. 2000; 162: 2259–2264. https://doi.org/10.1164/ajrccm.162.6.9812029.

[33] Orzechowska B, Awsiuk K, Wnuk D, Pabijan J, Stachura T, Soja J, *et al*. Discrimination between NSIP- and IPF-Derived Fibroblasts Based on Multi-Parameter Characterization of Their Growth, Morphology and Physic-Chemical Properties. International Journal of Molecular Sciences. 2022; 23: 2162. https://doi.org/10.3390/ijms23042162.

[34] Cecchini MJ, Hosein K, Howlett CJ, Joseph M, Mura M. Comprehensive gene expression profiling identifies distinct and overlapping transcriptional profiles in non-specific interstitial pneumonia and idiopathic pulmonary fibrosis. Respiratory Research. 2018; 19: 153. https://doi.org/10.1186/s12931-018-0857-1.

[35] Ligresti G, Raslan AA, Hong J, Caporarello N, Confalonieri M, Huang SK. Mesenchymal cells in the Lung: Evolving concepts and their role in fibrosis. Gene. 2023; 859: 147142. https://doi.org/10.1016/j.gene.2022.147142.

[36] Bergantini L, d'Alessandro M, Gangi S, Cavallaro D, Campiani G, Butini S, *et al*. Bronchoalveolar-Lavage-Derived Fibroblast Cell Line (B-LSDM7) as a New Protocol for Investigating the Mechanisms of Idiopathic Pulmonary Fibrosis. Cells. 2022; 11: 1441. https://doi.org/10.3390/cells11091441.

[37] Lehtonen S, Kaarteenaho R. Bronchoalveolar-Lavage-Derived Fibroblast Cell Lines Provide Tools for Investigating Various Interstitial Lung Diseases. Cells. 2022; 11: 2226. https://doi.org/10.3390/cells11142226.

[38] Burgy O, Mayr CH, Schenesse D, Fousekis Papakonstantinou E, Ballester B, Sengupta A, *et al*. Fibroblast-derived extracellular vesicles contain SFRP1 and mediate pulmonary fibrosis. JCI Insight. 2024; 9: e168889. https://doi.org/10.1172/jci.insight.168889.

[39] Lei Y, Zhong C, Zhang J, Zheng Q, Xu Y, Li Z, *et al*. Senescent lung fibroblasts in idiopathic pulmonary fibrosis facilitate non-small cell lung cancer progression by secreting exosomal MMP1. Oncogene. 2025; 44: 769–781. https://doi.org/10.1038/s41388-024-03236-5.